

## Seafloor expression of sediment extrusion and intrusion at the El Arraiche mud volcano field, Gulf of Cadiz

Pieter Van Rensbergen, Davy Depreiter, Bart Pannemans, and Jean-Pierre Henriët

Renard Centre of Marine Geology, Ghent University, Gent, Belgium

Received 4 May 2004; revised 1 October 2004; accepted 13 December 2004; published 24 May 2005.

[1] The El Arraiche mud volcano field consists of eight mud volcanoes up to 255 m high and 5.4 km wide, located in the Moroccan margin of the Gulf of Cadiz at water depths between 700 and 200 m. Available data include detailed swath bathymetry over the entire area, dense grids of high-resolution seismic data, very high resolution deep tow subbottom profiles, side scan sonar mosaics over the major structures, selected underwater video lines, and sediment samples. The main morphological aspects of the mud volcanoes are, from the margin toward the center, a subsidence rim or moat, the mud volcano slope, in some cases a deep crater, and a recent central mud dome at the top. The slope is characterized by radial outward sediment flow deposits or by a concentric pattern of terraces and steps. The sediment flow deposits can be divided into elongate outflows that accumulate at the base of the slope and short bulky outflow deposits that freeze on the steep slope. The crater hosts extruded sediment ranging from fluidized sand to mud breccia with centimeter- to meter-sized rock clasts issued from several vents within the crater. The concentric slope terraces and the central mud dome are interpreted to result from several phases of uplift caused by sediment intrusion or shallow diapirism. The mud volcano growth is thus interpreted to result from a combination of extrusive and intrusive processes.

**Citation:** Van Rensbergen, P., D. Depreiter, B. Pannemans, and J.-P. Henriët (2005), Seafloor expression of sediment extrusion and intrusion at the El Arraiche mud volcano field, Gulf of Cadiz, *J. Geophys. Res.*, 110, F02010, doi:10.1029/2004JF000165.

### 1. Introduction

[2] The El Arraiche mud volcano field (Figure 1) was discovered in May 2002 in the Moroccan Atlantic margin in the Gulf of Cadiz [Van Rensbergen *et al.*, 2005]. It consists of eight mud volcanoes of varying size and shape just below the shelf edge (Figure 2). The largest mud volcano in the field (Al Idrissi mud volcano) is 255 m high and 5.4 km wide. The 2002 surveys by the RV *Belgica* and the RV *Logachev* yielded detailed swath bathymetry over the entire area, dense grids of high-resolution seismic data, very high resolution deep tow subbottom profiles, side scan sonar mosaics over the major structures, selected video lines, TV grabs, dredge samples and gravity cores.

[3] The large amount of sea floor data and the clear shape of the larger mud volcanoes prompted this paper to focus on the morphology of the mud volcano cones. Although mud volcanoes are prominent features in the submarine seascape [see Kopf and Behrman, 2000, and references therein], little attention has yet been given to their small-scale morphology. Morphological mapping using high-resolution multibeam bathymetry offshore, or satellite altimetry onshore, has only become widely available during the past decade. Previously, submarine

mud volcanoes were imaged using side scan sonar mosaics and single beam bathymetry. The imaging resolution of deep towed side scan sonar systems is often an order of magnitude better than that of a hull-mounted multibeam system, but the impact of acoustic properties of the sediment and of the acquisition direction on the imaging makes it often difficult to interpret morphological information.

[4] Mud volcanoes in their broadest sense refer to any extrusion of mobilized sediment. Included are (1) mud volcanoes *sensu strictu* that are cone shaped with central vents, (2) mud mounds or ridges that are positive features without vent structure, and (3) mud pools that are negative features [Brown, 1990]. This morphological variation is related to the variation of fluid content [Shih, 1967], sediment properties and the width of the feeder system [Kopf and Behrman, 2000]. The feeder system may vary from narrow feeder pipes (diatremes) [Brown, 1990] that channel fluids and fluidized sediment to wide areas with bulk movement of plastic mud [Deville *et al.*, 2003]. Mud volcanoes *sensu strictu* are often considered as a sedimentary analog of stratovolcanoes, built by stacked sediment flows issued from a central crater or subsidiary vents at the flanks [e.g., Dimitrov, 2002]. In that case, outflow lenses accumulate as wedge-shaped deposits, thinning away from the feeder area, and build a mud volcano cone. The crater area is a low-relief area formed by collapse after expulsion of fluids and possibly

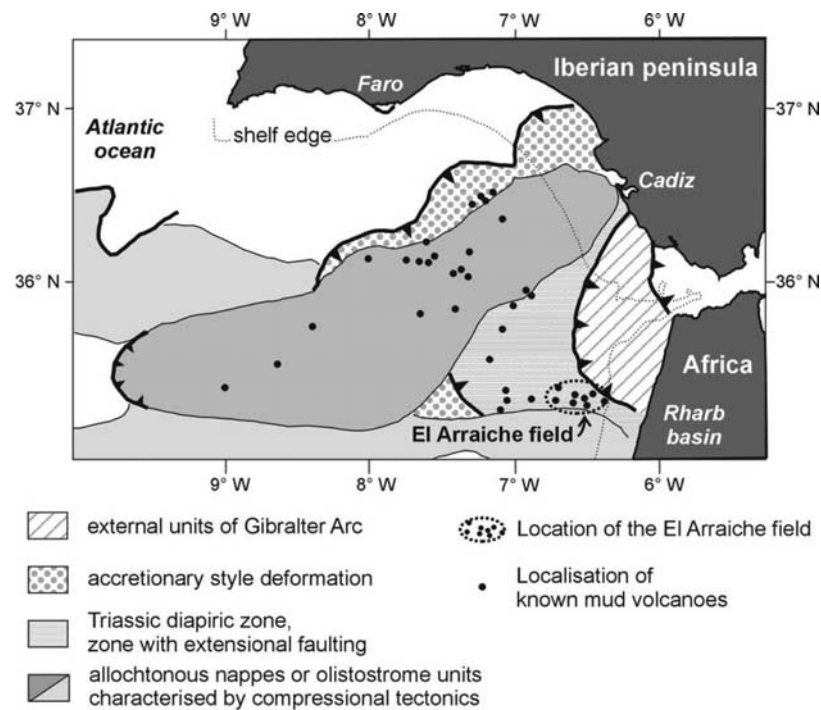


**Figure 1.** Geological setting of the El Arraiche mud volcano field, south in the Gulf of Cadiz (modified after Maldonado *et al.* [1999], Somoza *et al.* [2003], and Pinheiro *et al.* [2003]).

by subsidence because of sediment removal. As in the case for magmatic volcanoes [Annen *et al.*, 2001], the morphology of mud volcanoes *sensu stricto* is largely attributed to extrusion processes whereas the effect of intrusive processes remains unclear. High-resolution seismic profiles provide little information about the internal structure of a large mud cone, due to acoustic blanking.

We can in this case only deduce formation processes from the information available at the surface.

## 2. Geological Background

[5] In the Gulf of Cadiz, over 30 mud volcanoes have been sampled since they were first discovered in 1999

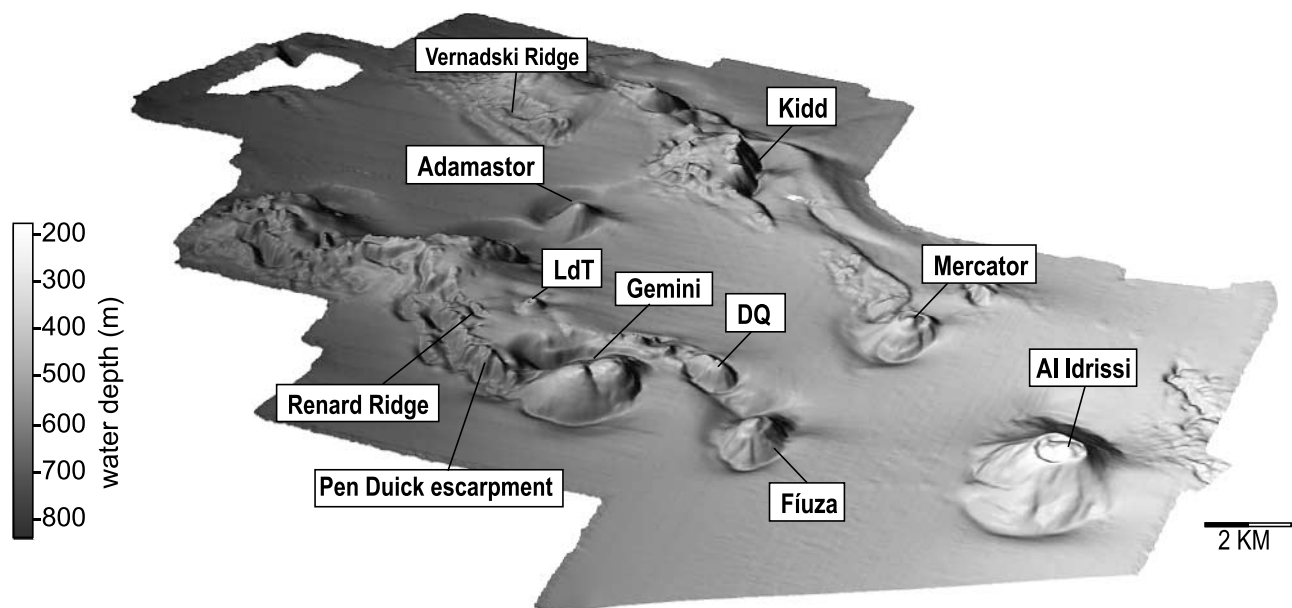


**Figure 2.** Three-dimensional morphology of the El Arraiche mud volcano field derived from multibeam bathymetry. Al Idrissi is the largest mud volcano, 255 m high and 5.4 km in diameter. Don Quichote (DQ) and Lazarillo de Tormes (LdT), the smallest mud volcanoes, are only about 25 m high.

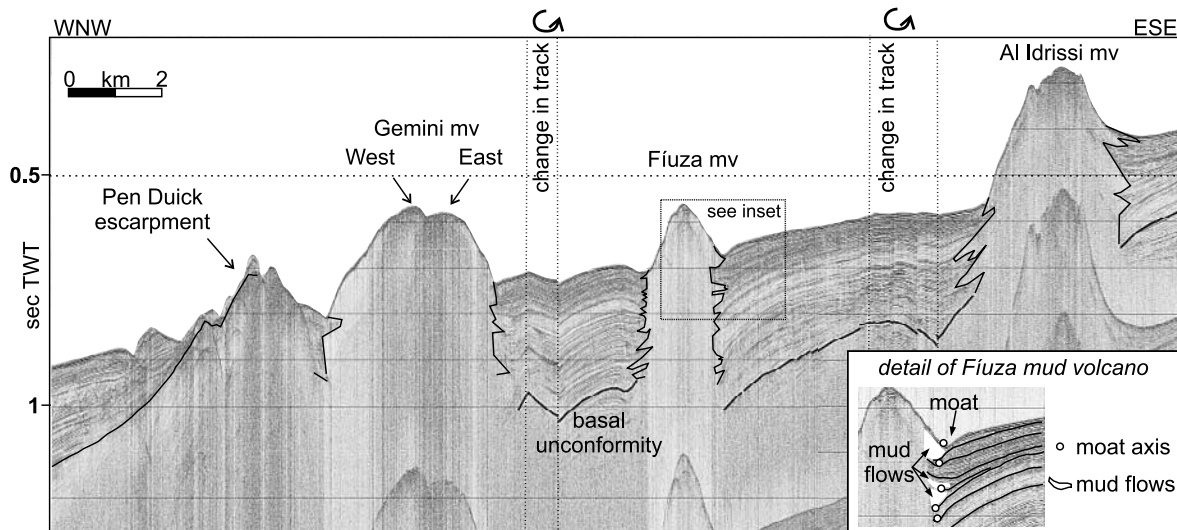


**Figure 3.** General high-resolution seismic line (sparker source) over Al Idrissi, Fúza, and Gemini mud volcanoes. On the seismic sections the mud volcanoes are reflection-free zones. At their flanks, mud flow deposits interfinger with stratified sediments. The inset shows a detail of interfingering mud flows that accumulate in moats at the base of the Fúza mud volcano cone.

[Gardner, 2001; *National Geographic*, 2002]. Most occur in the central part (Figure 1) [Somoza *et al.*, 2003; Pinheiro *et al.*, 2003] where large Miocene, densely faulted olistostrome units occur close to the sediment surface [Maldonado *et al.*, 1999]. The El Arraiche mud volcano field is located in the Moroccan Atlantic continental slope in water depths ranging from 200 m to 700 m. In contrast to the central mud volcano fields, the El Arraiche field is located over a large extensional Pliocene basin between regions of olistostrome emplacement (Figure 1) [Flinch, 1993; Flinch *et al.*, 1996; Gràcia *et al.*, 2003]. Within the Pliocene basin, the El Arraiche mud volcanoes occur over anticlinal ridges where the Pliocene plumbing system is thinnest and extensional faulting facilitates fluid and sediment injection into the overburden [Van Rensbergen *et al.*, 2005]. On seismic sections (Figure 3), the mud volcanoes are imaged as a columnar zone without acoustic penetration, about the width of the mud volcanic cone. Large sediment flows emerging from this central zone are also free of reflections, but show a sharp transition to the stratified hemipelagic sediment. These sediment flows are typically lens shaped, convex at the top and often fill a moat at the base of the mud volcano. The earliest sediment flows occur just above a regional unconformity, about 350 m and 900 m below sea level, attributed to a sea level low at 2.4 ma [Hernández-Molina *et al.*, 2002; Van Rensbergen *et al.*, 2005]. Since this time successive episodes of mud volcanism created a pile of remolded mud of over 400 m thick.

### 3. Data and Methods

[6] The multibeam survey on board R/V *Belgica* used a Kongsberg EM 1002, extended with a deep water module. Maximum sailing speed was 6 knots, with a swath width of 750 m in shallow water (<500 m) and limited to 500 m in deep water to reduce signal deterioration and noise. The acquired data were corrected and cleaned with the Kongsberg packages Merlin and Neptune. The footprint at 400 m

is 15 m × 15 m. In total, 700 km<sup>2</sup> were covered. In addition, a total of 62 high-resolution seismic profiles were acquired in three dense grids with a line spacing of about 1 km centered on the Mercator, Al Idrissi and Gemini mud volcanoes [Van Rensbergen *et al.*, 2005].



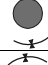


[7] During the TTR 12 survey, side scan sonar imagery over the main features was acquired using the deep-towed hydroacoustic complex Mak-1, with an operating frequency of 30 kHz, and a subbottom profiler operating at 5 kHz. On the basis of the side scan sonar data, six transects were chosen for a deep-towed video line, for a total of 15 hours. On the basis of the video lines, TV-guided grab samples were taken. Dredge samples of mud breccias at the surface were taken on Mercator and Al Idrissi mud volcanoes. In the craters of the main mud volcanoes (Mercator, Al Idrissi, Gemini, and Fúza) the subsurface was sampled by gravity cores. Four additional box cores are also available from the R/V *Belgica* survey.

[8] From the eight mud volcanoes in the cluster, four (Al Idrissi, Mercator, Gemini and Fúza) are studied in detail by combining multibeam, side scan sonar and sedimentological data. For a better visualization, slope angle and curvature (second derivative of  $z$  in  $x$  and  $y$ ) were calculated on basis of the three-dimensional bathymetry. The curvature function calculates isobath curvature on a map view and distinguishes between convex and concave shapes. It is a good tool to map sediment flow deposits as they stand out as elevations (convex) on the slope. The sedimentary facies within the crater and on the upper slopes were described from underwater video lines calibrated by core, dredge and grab samples.

### 4. Data Description and Interpretation

[9] The morphology of the mud volcanoes in the El Arraiche field consist of, from base to top: a moat around part of the base of the mud volcano cone, an irregular slope characterized by radial outward sediment flows,



name	Water depth top (m)	Height (m)	Slope			Crater max depth (m)	Crater's central dome		Moat		
			Width base (km)	Width top (km)	Overall angle (°)		Height (m)	Diameter (km)	Radius (km)	Max depth (m)	Quadrant
<b>Al Idrissi</b>	197	111 - 255	4.3 - 5.4	1.2 - 1.5	5 - 8	17	14 - 42	1.9 - 2.3	2.85	16	
<b>Mercator</b>	350	51 - 141	2.45 - 1.82	0.98 - 1.1	5.5 - 10	2	22 - 38	0.65 - 0.8	1.3	9	
<b>Gemini W</b>	423	170 - 252	4.1 - 2.3	1.1	5.5 - 8.5	No crater	23 - 27	0.52 - 0.87	1.5 - 1.9	12	
<b>Gemini E</b>	423	117 - 169		0.95 - 1.3	5 - 10.5	No crater	13 - 23	0.7 - 0.87	0.95 - 1.25	3	
<b>Fiuza</b>	393	97 - 143	2.9 - 2.1	0.75 - 0.8	6 - 10	No crater	27	0.5 - 0.7	1.1 - 1.6	36	

**Figure 4.** General morphological characteristics of the main mud volcanoes of the El Arraiche field.

terraces and/or depositional sediment flow escarpments (lobe fronts), a crater depression or a flat top, and a central dome. Figure 4 gives an overview of the measures of these main morphological aspects for the mud volcanoes discussed in this paper. More detailed measurements are listed in Table 1 to avoid lengthy descriptions in the next paragraphs.

#### 4.1. Al Idrissi Mud Volcano

[10] Al Idrissi mud volcano is the largest and shallowest mud volcano in the field, situated just below the shelf edge (Figure 5). It is up to 255 m high and 5.4 km in diameter. It has a well-developed crater (−17 m) and large central dome (42 m) within the crater. Numerous sediment flow deposits characterize the flanks of the mud volcano (Figure 5a) and extend from the crater to the moat at the base. The moat is up to 16 m deep and has a radius of about 2.85 km. On side scan sonar data, high-backscatter sediment flow deposits contrast sharply with the low-backscatter sea floor (Figure 5b), except at the southeastern side of the volcano where the backscatter intensity weakens probably due to a thickening hemipelagic cover. The contrast in backscatter distinguishes erupted sediment from the hemipelagic slope sediments. Sediment extrusion is well constrained to the semicircular cone. There are no distant outrunners observed. The radial pattern of down slope sediment flows is clearly visualized by the curvature function (Figure 5c).

[11] Two types of sediment flow deposits can be distinguished: elongated sediment flow deposits that extend to the foot of the slope (type I) and short bulky sediment flow deposits that occur on the steeper parts of the slope (type II). Type I sediment flow deposits are up to 2.5 km long and accumulate at the foot of the slope in a fan or drop-shaped termination. Their distal part is often captured and deflected by the erosional moat. They have an even texture on side scan sonar indicating a smooth surface without flow fronts. The slope has a concave profile with an increasing slope angle of  $0.5^{\circ}$ – $7^{\circ}$  at the base to  $12^{\circ}$ – $14^{\circ}$  near the top (Figure 5d). Type II sediment flow deposits occur mainly at the western slope in a somewhat tongue-shaped area with irregular relief. They do not extend downward to the base of the slope. The depositional lobes have a very steep and high depositional fronts ( $<14^{\circ}$ ). The

resulting slope is irregular but with a constant overall angle of about  $8^{\circ}$ .

[12] The crater and the top of the slope of Al Idrissi mud volcano (Figure 6) were surveyed with underwater video lines and sampled by gravity cores, box cores and dredges. Within this area two sedimentary facies can be identified; AI-1 and AI-2. Facies AI-1 is a coarse, pebbly sand with some patches of small stones ( $<10$  cm) that covers most of the crescent-shaped crater depression and the central cone within the crater (Figure 5e). Core 411G and box cores B1 and B2 (location in Figure 6b) at the top and at the northern flank of the central dome reveal that the sandy layer is only 3–5 cm thick with a sharp and irregular limit separating it from mud breccias. In core 411G (Figure 7) this mud breccia is a stiff, structureless clay with clay stone clasts up to 1 cm. Facies AI-2 is the main facies on the slopes within and around the crater and is very heterogeneous. Stones litter the surface, with sizes ranging from 1–2 cm to more than 50 cm. Clast distribution ranges from areas featuring virtually no stones, strongly resembling AI-1, to true piles of blocks. A dredge over AI-2 at the upper western slope showed that the stones have a wide variety of lithologies, from cemented limestone to sandstone. On the southeast slope, prominent features of facies AI-2 are smoothed by a drape of dark green mud. Facies AI-2 and AI-1 are interpreted as material that was brought to the surface by mud volcanic extrusion, with possible reworking and redistribution of sediment within the crater. The crater sedimentology contrasts strongly with the background sediment, which was retrieved in box core B3 (Figure 5e), north of Al Idrissi at 415 m water depth and consists of a homogenous light brownish oxidized mud (silty clay).

[13] Sediment extrusion in the crater is imaged in detail using the curvature function in combination with side scan sonar (Figure 6a) and sedimentological data from video lines and sea floor samples (Figure 6b). Sediment flows within the crater were erupted from at least three individual vents. Vents are interpreted to be present at the common origin of radial sediment flow deposits, often a rounded elevation. Sediment flows from vent A and B are associated with the rocky sediment facies AI-2 and display a series of flow fronts on side scan sonar images that are below the resolution of the multibeam system. The sandy facies AI-1 is associated with flows from vent C at the top of the central

**Table 1.** Detailed Measurements of the Main Morphological Elements of the Mud Volcanoes

Interpreted Extrusion Types	Slope Profile	Overall Slope Angle, deg	Steepest Depositional Slope Angle, deg	Lowest Depositional Slope Angle, deg	Lobe Fronts and Terraces		
					Maximum Height, m	Maximum Width	Distance From Crater Rim, km
Type I elongate mud flows	steepening concave-up straight with undulations terraced	5 (incl. by-pass zone) 8 3	8.5 14 7.5	0.5 4 0 at top	~20 ~40 ~10	~800 ~700 ~700	0.9–2.5 0.45–1.4 within crater
Type II short mud flows							
Crater's central dome							
Type I elongate mud flows	steepening concave-up terraced convex -up	5.5 8 5	8 12.5 11	1.5 2.5 0 at top	no lobe fronts ~45 ~25	~600 ~1500 ~500	0.9–1.3 0–1 within crater
Diapiric uplift?							
Crater's central dome							
Type I elongate mud flows	steepening concave-up terraced, convex-up terraced convex -up	5 8.5 10.5 3	10 15.5 17 9.5	1 5.5 6 0 at top	no lobe fronts ~45 ~35 ~20	~600 ~600 ~1400 ~500	0.8–1.2 0.25–0.9 0–1.1 within crater
Type II short mud flows							
Diapiric uplift?							
Crater's central dome							
Type I elongate mud flow	steepening concave-up terraced, convex-up terraced convex -up	6 10 8 2.5	10 18 13 6	5 6 3.5 0 at top	~15 ~50 ~30 ~10	~600 ~400 ~400 ~200	0.6–0.9 0.3–0.7 0–0.8 within crater
Type II short mud flows							
Diapiric uplift?							
Crater's central dome							

dome. Most likely, fluidized sand spread out from the top to the deepest part of the crater depression. The sand layer is only 3–4 cm thick and it is unlikely that it formed the observed convex sediment flow deposits, which has meter-scale relief. Therefore it is interpreted to postdate earlier mud breccia extrusion at vent C.

#### 4.2. Mercator Mud Volcano

[14] Mercator mud volcano is an asymmetric mud volcano (Figure 8), about 140 m high at the southern side but only 90 m high at the northern side and only 50 m high at the eastern side. The crater is very shallow (–2 m) but the central dome is large (38 m). In this case, the slope is characterized by concentric steps rather than by radial sediment flow deposits.

[15] The concentric pattern is mainly caused by two terraces at the southern flank of the mud volcano (Figure 8). These terraces are almost horizontal (slope 2°–3°) separated by high steps that continue laterally for up to 1.5 km. The overall slope of the southern flank is about 7°. The upper slope has a high backscatter on side scan sonar data that is not related to the step-like morphology but probably caused by lithology or surface roughness. Flow fronts on the side scan sonar image coincide with short convex deposits that may be attributed to type II sediment flows. These sediment flow deposits are difficult to distinguish and do not seem to have a large effect on the overall slope morphology.

[16] Type I sediment flow deposits fan out at the base of the western slope (Figure 8). They extend 1300 m from the crater edge and accumulated in a base-of-slope deposit. Depositional lobes (on the scale of the available resolution) have a width of 500–600 m. The depositional slope is very low (1°–2°) and there are no steep flow fronts observed. On side scan sonar data (Figure 8b), these sediment flow deposits have a smooth surface and a low backscatter that blends in with the surrounding sea floor. The northern flank is a steep regular and smooth surface with a slope of about 10°–13°. An escarpment at the eastern flank could be related to a WNW-ESE oriented fault, which would help to explain the asymmetry in the morphology. No such fault was observed on the subsurface data. The escarpment may be due to gravitational instability of the southern mud volcano flank (G. Ernst, personal communication, 2004), but no such indications were observed on the subsurface data.

[17] The top of the Mercator mud volcano (Figure 9) consists of a shallow crater (–2 m) and high central dome (38 m). At the southern side the crater is absent and only a break in slope occurs. The central dome is flat topped with an overall slope of about 5°. Mud breccia with up to 10 cm large clasts crops out at the sea floor at the top of the central dome. On the basis of underwater observations and sediment samples, a generally decreasing thickness of the hemipelagic mud overlying the mud breccia is observed from the flanks toward the top. The hemipelagic sediment cover has a thickness of 8 cm at core 408G (Figure 7). At the top of the central dome a single vent was identified at the origin of radial sediment flow deposits within the crater. The sediment flow deposits are characterized by concentric flow fronts on side scan sonar data that seem to culminate in steep slope at the front of the depositional

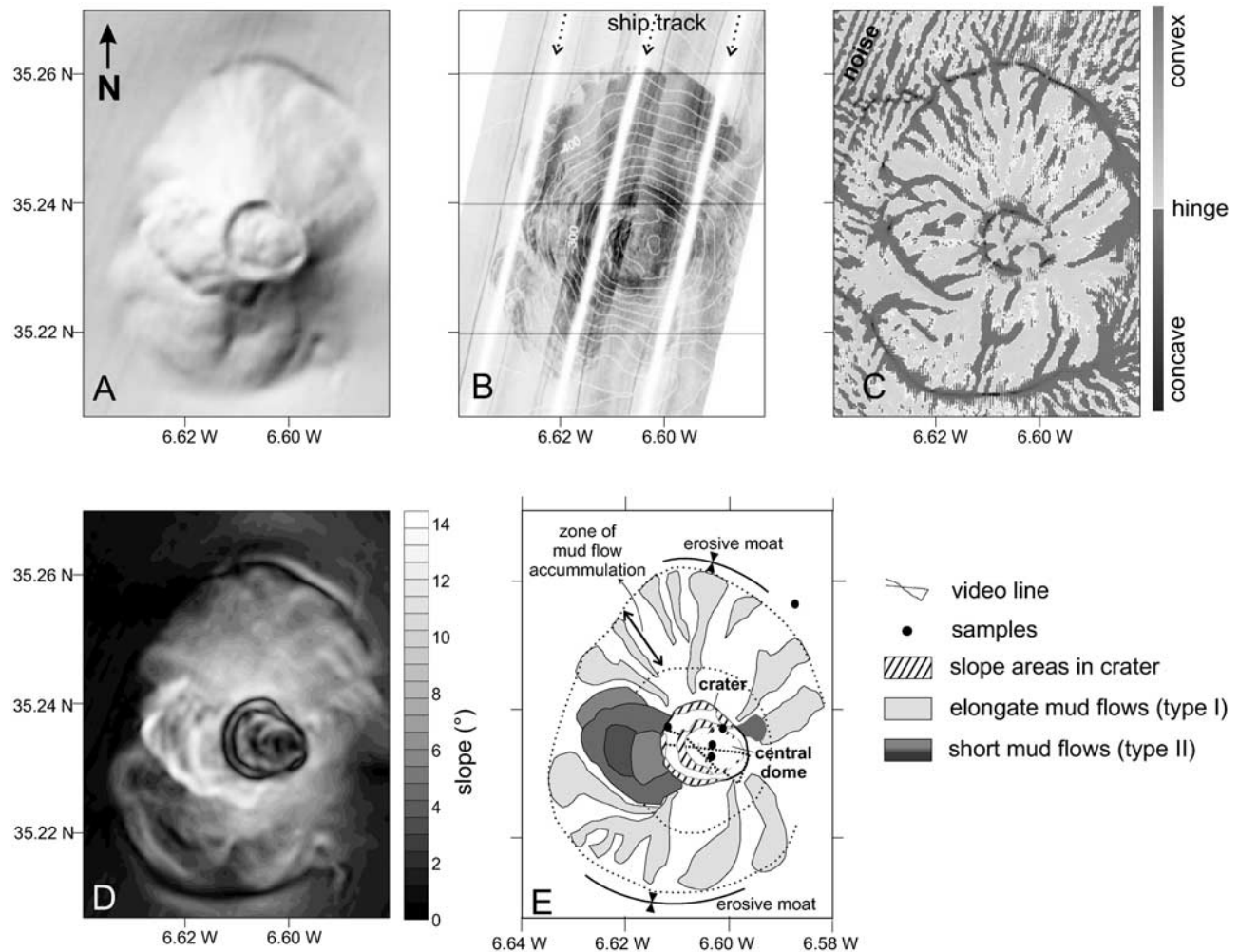


**Figure 5.** Morphology of the Al Idrissi mud volcano. (a) Shaded relief map. (b) Side scan sonar mosaic with bathymetry contours. (c) Curvature of mud volcano isobaths. (d) Slope map with bathymetry contours. (e) Interpretation map. Numerous sediment flow deposits, characterized by high backscatter and convex morphologies, are distinguished on the slopes. They occur in a radial pattern away from the crater and accumulate at the base of the volcanic cone (type I sediment flows), which results in a steepening, concave slope profile. On the western slope, sediment flow deposits accumulated at the slope (type II sediment flows) and created a steeper irregular slope profile. See color version of this figure at back of this issue.

lobe. These extrusive deposits are also covered by hemipelagic mud, except at the top of the central dome. The most recent extrusion was restricted to the crest of the central dome, which indicates that extrusive activity has been decreasing. This is confirmed by low hydrocarbon seepage activity assessed by *Van Rensbergen et al.* [2005].

#### 4.3. Gemini and Fúza Mud Volcanoes

[18] Gemini mud volcano consists of two summits in one large oval-shaped mud volcano (Figure 10). The Gemini mud volcano is about 250 m high, 4.88 km long to 2.5 km wide at the base, the diameter at the top of the eastern part is 0.9 km and the diameter of the western part is 0.6 km. The summits consist of a flat area with central domes of 23 m and 27 m, respectively, above the flat top. The differentiation between the two summits is visible from about 80 m below the top of the mud volcano as a 400 m long and 20 m deep crease.

[19] The morphology of the slopes involves semiconcentric terraces at southern and northwestern flanks, type I sediment flow deposits at the eastern and western sides, and, less distinguishable, type II sediment flow deposits at the northern slope of Gemini East. The semiconcentric steps are about 20 m high, have a maximum slope of  $17^\circ$ , and continue laterally for about 1–1.4 km. At the northern flank of Gemini East, the steps are only 500 m wide and may also be attributed to type II sediment flow deposits. The side scan sonar data show high backscatter and irregular texture, similar to the upper slopes of the Mercator mud volcano. Type I sediment flow deposits are only visible at the eastern and western sides of the mud volcano. They are characterized by the fan-shaped deposit at the base of the slope, and their smooth texture and low-backscatter values on side scan sonar data.

[20] The sedimentology of the top of the mud volcano is similar to that of the Mercator mud volcano and consists of



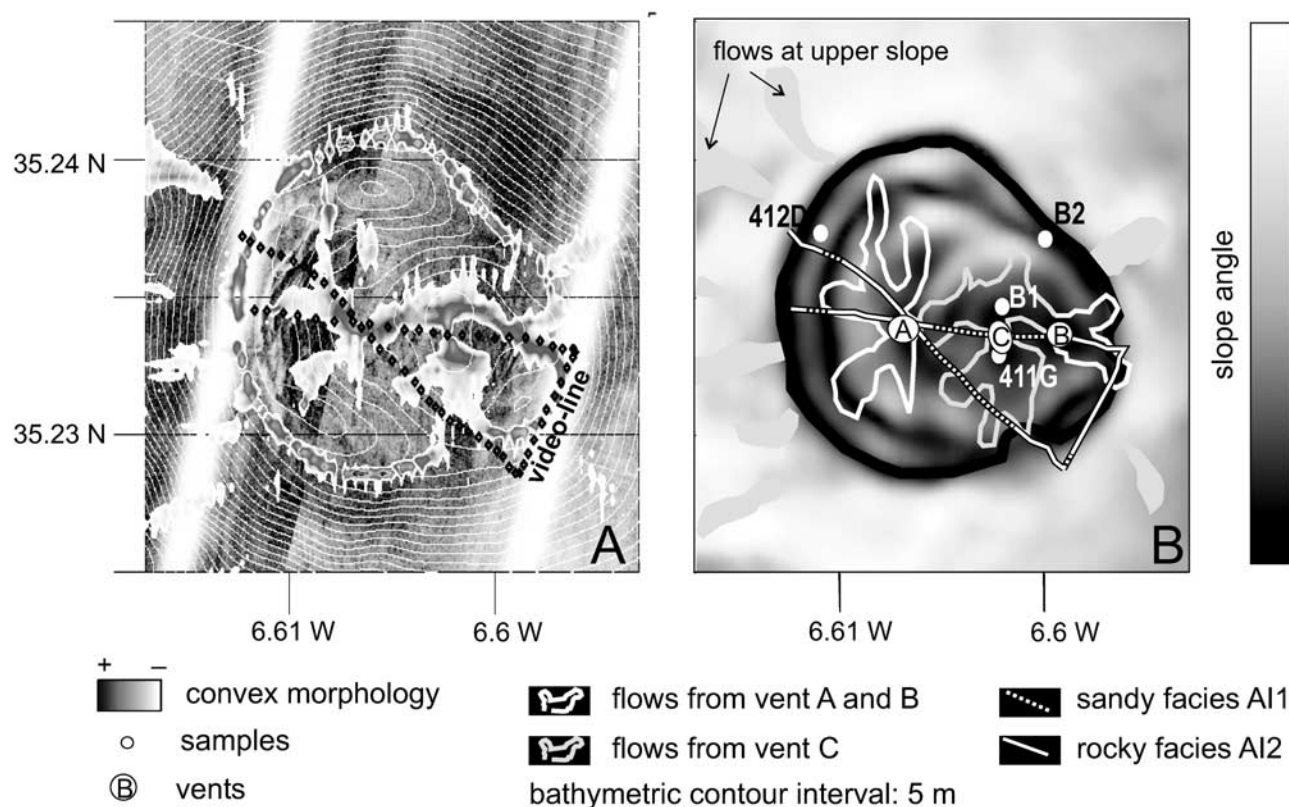


**Figure 6.** Crater of Al Idrissi mud volcano. (a) Convex morphologies mapped over side scan sonar image shows the distribution of small mud flows issued by vents within the crater. (b) Slope map with indication of interpreted sediment flow deposits and sedimentary facies from underwater video lines distinguishing the different outflow events. See color version of this figure at back of this issue.

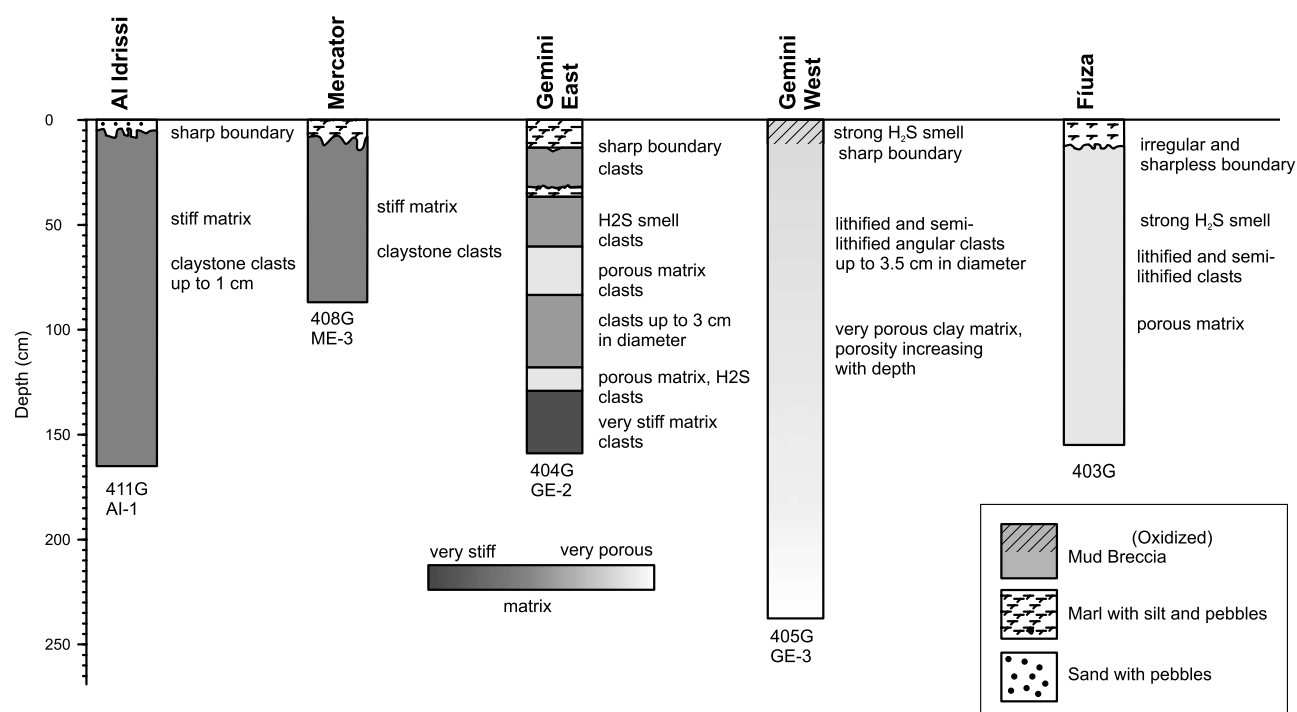


**Figure 7.** Description of gravity cores located at the crests of the main mud volcanoes. The localization of the cores is indicated in Figure 6 (crater of Al Idrissi mud volcano), Figure 9 (crater of Mercator mud volcano), Figure 10 (for Flúza mud volcano), and Figure 11 (top of Gemini mud volcano). Cores have widely varying fluid contents. Inactive mud volcanoes are covered by a hemipelagic drape.

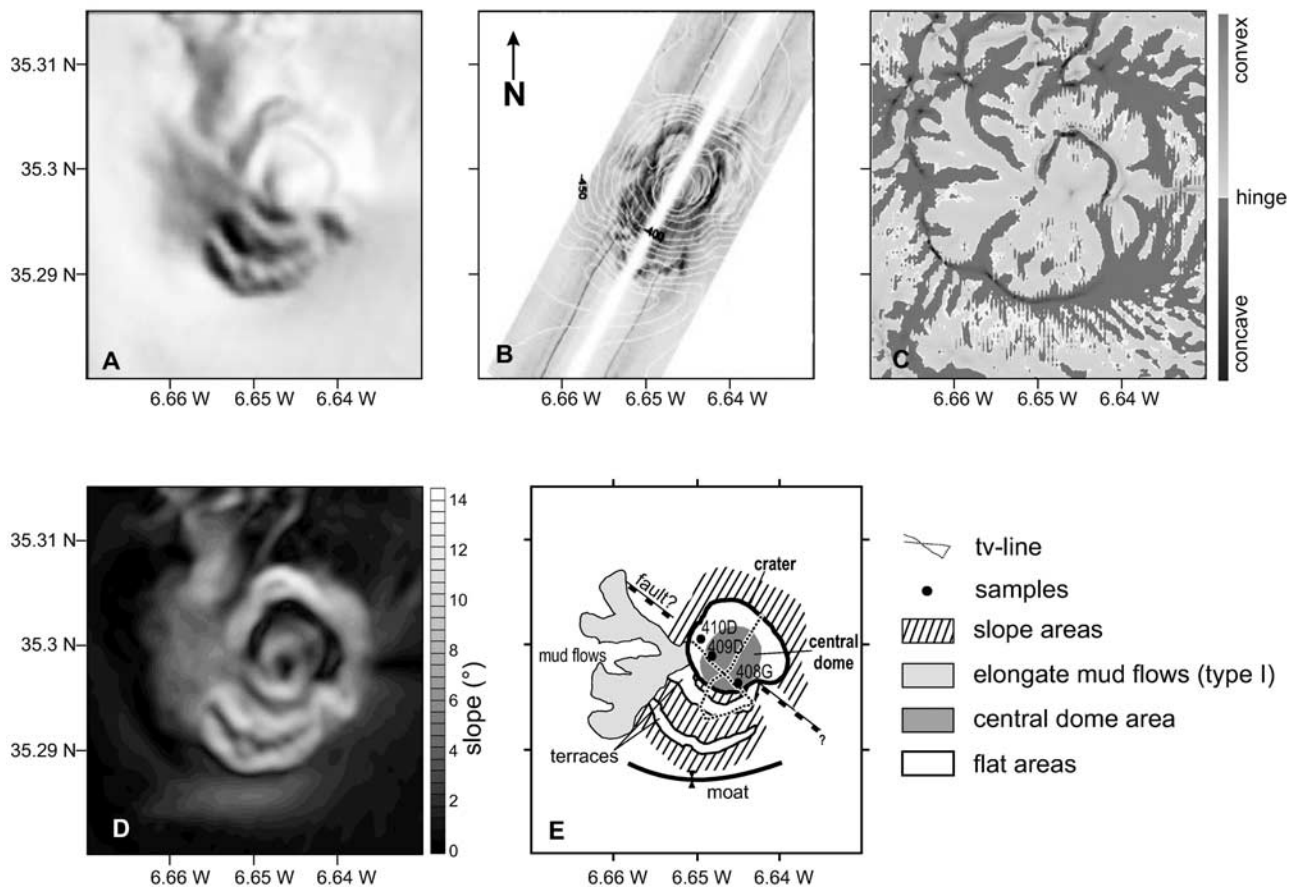


**Figure 8.** Morphology of the Mercator mud volcano. (a) Shaded relief map. (b) Side scan sonar mosaic with bathymetry contours. (c) Curvature of mud volcano isobaths. (d) Slope map with bathymetry contours. (e) Interpretation map. Mercator mud volcano is an asymmetric mud volcano with a smooth northern slope and concentric steps at the southern slope. Only at the western slope, type I sediment flow deposits, here characterized by a low backscatter, fan out at the base of the cone. See color version of this figure at back of this issue.

mud breccia overlain by hemipelagic mud of varying thickness. Core 404G at the eastern summit (Figure 7) reveals 12 cm of bioturbated marl (hemipelagic mud), on top of different layers of mud breccias. Core 405G at the western summit (Figures 7 and 10e) shows a gray mud breccia with a heavy  $H_2S$  smell without hemipelagic sediment. The surface layer is an oxidized, heavily bioturbated mud breccia with centimeter-sized clasts. Figure 11 shows the detail of the top of the mud volcano. Sediment flow deposits issued from at least six vents distributed over the crestal area were identified. A remarkable observation is that the gully that separates both crests is not filled in by the extrusive sediment flows.

[21] Fiuza mud volcano is a smaller mud volcano east of Gemini (Figure 10). It is 143 m high, up to 2.9 km wide at the base and has a flat top of about 800 m wide with a central dome of 27 m high and 500–700 m wide. The flanks of the Fiuza mud volcano mainly consist of radial outward type I sediment flows with an overall slope of about  $6^\circ$ . At the northern flank (overall slope about  $9.5^\circ$ ), a 400 m wide step with a slope of  $18^\circ$  may be attributed to a type II sediment flow. At the southern flank (overall slope  $6.5^\circ$ ) a series of steps with a slope of about  $11^\circ$  resemble the

morphology that typified the Mercator mud volcano. Core 403G (Figures 7 and 10e) at the top of the mud volcano retrieved a homogeneous mud breccia covered by 12 cm of pelagic marl. The Fiuza mud volcano is encircled by a moat with a maximum depth of 27 m below the surrounding sea floor. The Fiuza mud volcano is too small for its summit to image successfully.

## 5. Synthesis and Discussion

### 5.1. Extrusion Deposits

[22] In a synthesis of our observations (Figure 12) four types of sediment extrusion deposits could be distinguished. Table 2 is a synthesis of Table 1 and gives the measured minimum and maximum values for each morphological element.

[23] 1. Type I sediment flows form elongate concave deposits that spread out at the base of the slope. The smooth, even texture stands out on side scan sonar data, also when the backscatter is high. They are characterized by low depositional slopes, gentle lobe fronts (if any) and a long down slope length. As they accumulate at the base of the slope they tend to reduce the overall slope angle and



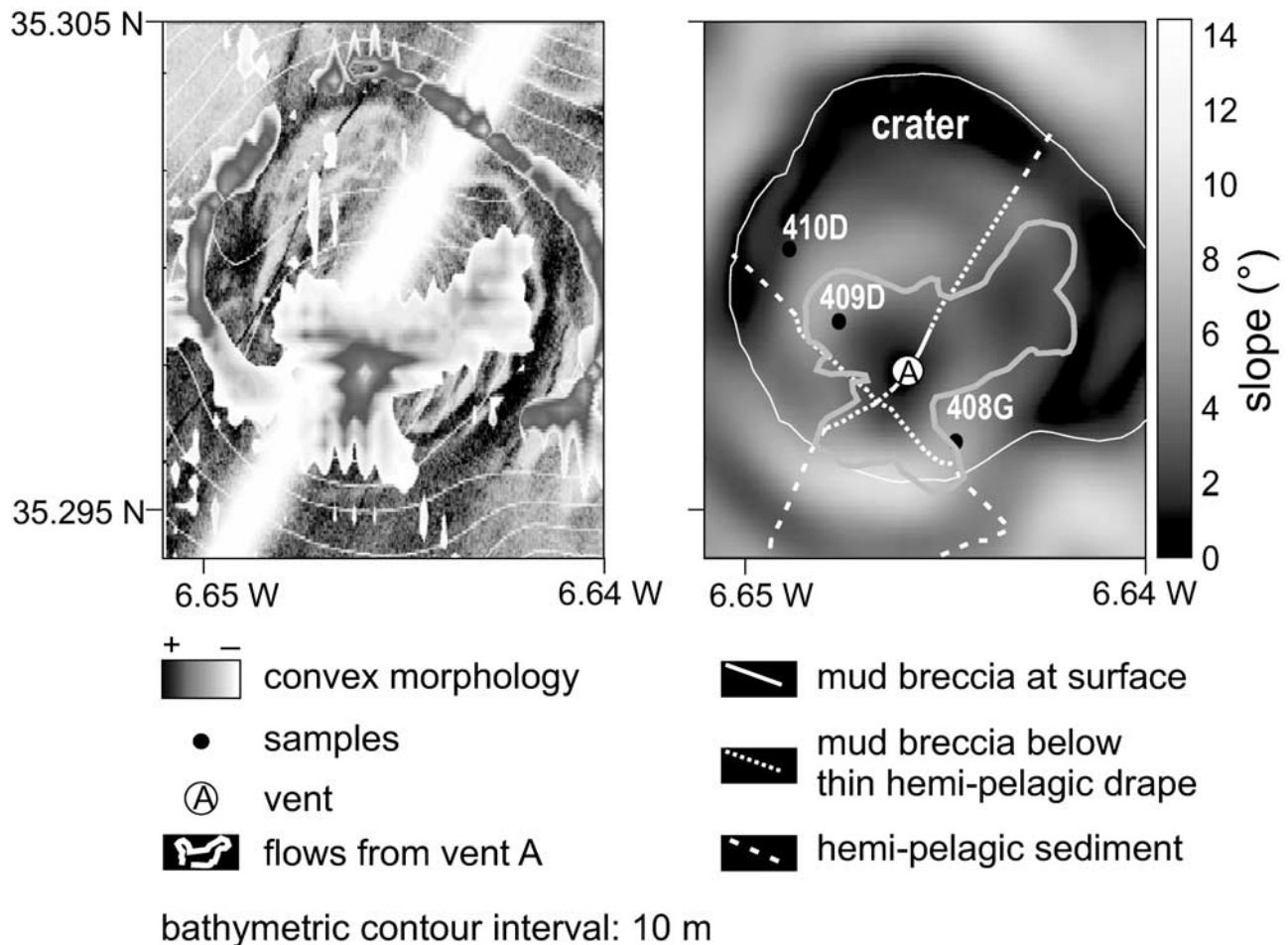


**Figure 9.** Crater of Mercator mud volcano. (a) Convex morphology mapped over side scan sonar image shows the distribution of small mud flows within the crater around a single vent at the summit. (b) Slope map with indication of interpreted sediment flow deposits and sedimentary facies from underwater video lines. See color version of this figure at back of this issue.

create a typical steepening concave slope profile. They can be interpreted as debris flows with low yield strength [Mulder and Cochonat, 1996].

[24] 2. Type II sediment flows form short irregular flow deposits that accumulate on the mud volcano slopes. Semiconcentric flow fronts, variable backscatter and irregular texture characterize type II flow deposits on side scan sonar data. The depositional slopes are considerably steeper and lobe fronts are high. The resulting slope profile is irregular with a linear to convex profile. They can be interpreted as debris flows with high yield strength [Mulder and Cochonat, 1996].

[25] 3. A third type of debris flows is restricted to the crater area. Several vents at the top and the flanks of the central dome issue small-scale debris flows but do not evolve into large eruptions feeding large down slope sediment flows. This is the most recent extrusion activity at the mud volcanoes [Van Rensbergen et al., 2005]. They consist of mud breccia with centimeter- to meter-sized clasts. It is not possible to determine whether they are the equivalent of type I or type II sediment flows.

[26] 4. A fourth type of sediment extrusion is fluidized sand ejection. Fluidization only occurs in cohesionless

sediments and is different from the cohesive mud breccia flows. Extrusion of fluidized sand may account for the sand layer at the top of the Al Idrissi mud volcano. Sand layers were also encountered at the top of the Kidd mud volcano (Gulf of Cadiz) [Gardner, 2001] and in the crater of the Granada mud volcano [Kenyon et al., 2000].

[27] The above four types are sediment extrusion features that shape the surface of the mud volcanic cone. The processes of sediment extrusion and some geomechanical aspects have been discussed by Henry et al. [1996] and Kopf and Behrman [2000] for mud volcanoes respectively offshore Barbados and at the Mediterranean Ridge. Both manuscripts describe the ascending mud as a low-viscosity fluid that is injected along narrow diatremes or conduits. The size of the clasts it carries to the surface is thought to depend on the velocity of the liquid mud. Nevertheless, our observations provide evidence for the variability in extruded sediment (sand to mud breccia with centimeter- to meter-sized clasts and varying porosity) within one mud volcano. Subsequently, differences in debris flow accumulation cause variations in the growth processes from widening and flattening of the cone (type I flows) to

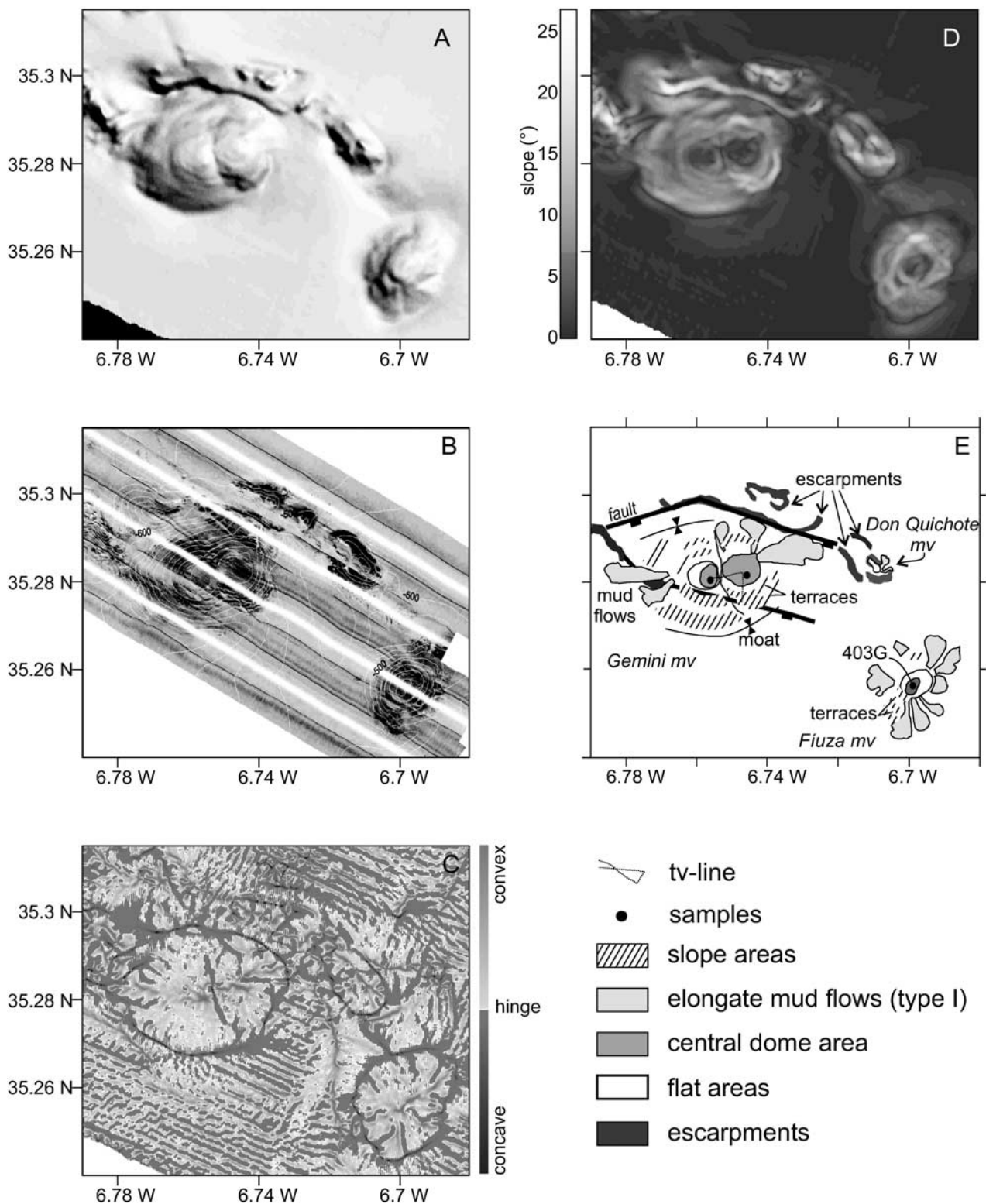


**Figure 10.** Morphology of Gemini and Fiuza mud volcanoes. (a) Shaded relief map. (b) Side scan sonar mosaic with bathymetry contours. (c) Curvature of mud volcano isobaths. (d) Slope map with bathymetry contours. (e) Interpretation map. Gemini mud volcano is a large oval-shaped mud volcano with two summits and an overall convex slope profile. The northern and southern flanks are steep with semiconcentric terraces. Type I sediment flow deposits at the base of the eastern and western slopes locally decrease the steep slope gradient. The flanks of the Fiuza mud volcano mainly consist of radial outward type I sediment flows that appear to mask a series of steps at the southern flank. See color version of this figure at back of this issue.

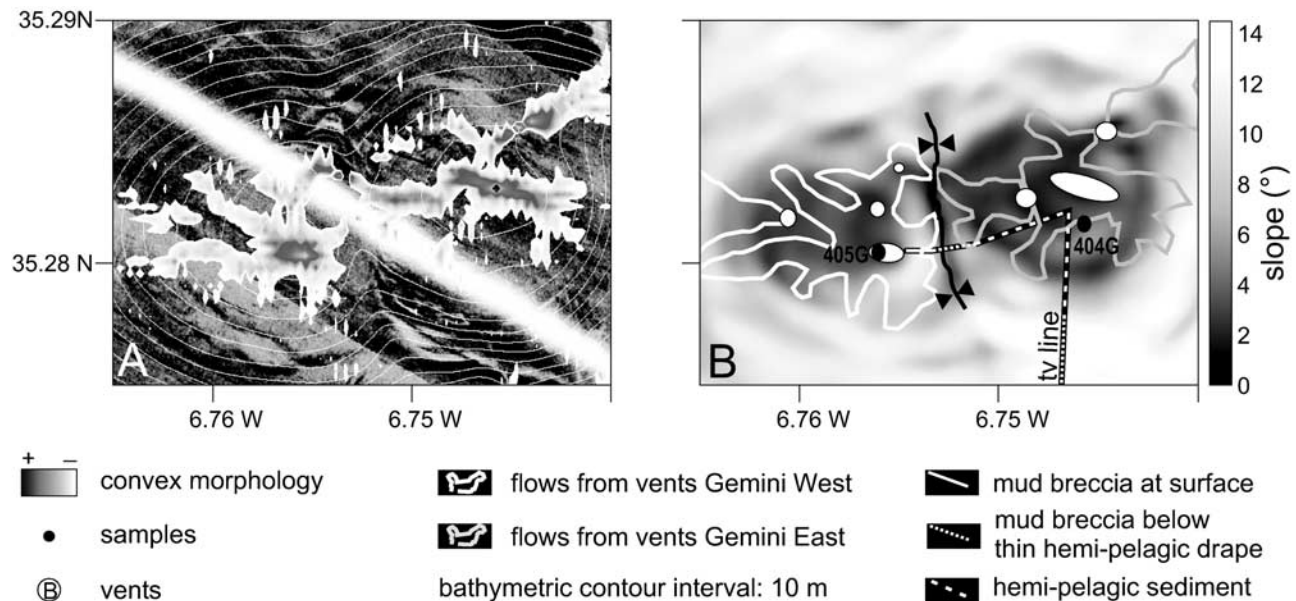


**Figure 11.** Crater of Gemini mud volcano. (a) Convex morphology mapped over side scan sonar image. (b) Slope map with indication of interpreted sediment flow deposits and sedimentary facies from underwater video lines. Up to seven vents have been identified at both summits. At the western summit, mud flow extrusion occurred recently. See color version of this figure at back of this issue.

steepening of the slopes by cohesive debris flows (type II flows).

## 5.2. Endogenic Processes

[28] Mud volcano growth is not only controlled by the obvious exogenic processes but also by less conspicuous endogenic processes. According to *Brown* [1990] and *Camerlenghi et al.* [1995], mud volcano cones are formed during last phase mud volcano activity by intrusion of mobilized sediment, after an episode of mainly fluid and gas expulsion in mud pools. In this study we also observe morphological elements that do not appear to correspond solely to extruded sediment deposits and may partly result from endogenic growth processes.

[29] 1. The elevation of the central dome in the crater hosts several vents extruding small sediment flows. The overall slope of the central dome is much less steep than the slope of the mud volcano flanks. The central domes consist of mud breccia with varying matrix density. In all mud volcanoes of the El Arraiche field, the central dome is the youngest morphological feature, postdating sediment flows on the slopes.

[30] 2. A concentric pattern of terraces and steps is observed at Mercator, Gemini and Fiuza mud volcanoes. The terraces and steps have a large along slope continuity. The steps are less high and less steep than the lobe fronts created by type II sediment flows. The resultant slope has a step-like, concave profile. The typical step-like slope may be obliterated later by extrusive sediment flows and may evolve into a linear (type II flows) or steepening concave (type I flows) slope profile.

[31] The central dome, the concentric terraces and steps are most likely not formed by lobes of extruded debris flows but are attributed here to diapiric phases, possibly followed by collapse. Uplift of the sedimentary overburden by

diapirism may occur by vertical pressure exerted by a buoyant diapiric body and/or by the injection of sedimentary dykes and sills [*Annen et al.*, 2001]. Mud diapirism driven by density reequilibration is likely to occur within the mud volcano edifice. Variations in gas and fluid content can create large density differences in the mud. For example, *Kopf and Behrman* [2000] measured mud breccia densities of mud volcanoes at the Mediterranean Ridge ranging between 1200 and 1400 kg m<sup>-3</sup> for mousse-like silty and sandy clays to 1700–2300 kg m<sup>-3</sup> for matrix supported mud debris flow deposits. A simple calculation of the possible gravitational compensation using the above values indicates that a central dome of 40 m height has an isostatic compensation depth of maximum 90 m below the top of the mud volcano. In other words, buoyancy effects within the mud cone can cause internal diapirism, even without taking into account the effect of elevated fluid pressure. Shallow-seated diapirism that extruded mud cones at the sediment surface without much sediment fluidization (small fluid and gas flux) was documented in Lake Baikal and contrasted sharply with neighboring gas and fluid expulsion craters caused by a large gas flux [*Van Rensbergen et al.*, 2003].

[32] On a larger scale, the same process may occur within the 400-m-thick pile of remolded sediment that accumulated since the onset of mud volcanism about 2.4 ma ago [*Van Rensbergen et al.*, 2005]. The concentric pattern of terraces and steps may be caused by successive diapiric phases with decreasing diameter, each possibly followed by collapse and crater formation due to degassing or dewatering. Similar terraces on the slope of the Ginsburg mud volcano, west of the El Arraiche mud volcano field, were interpreted by *Gardner* [2000] as a diapiric feature.

[33] The occurrence of uplift and diapirism in mud volcanoes seems contradictory to their common association



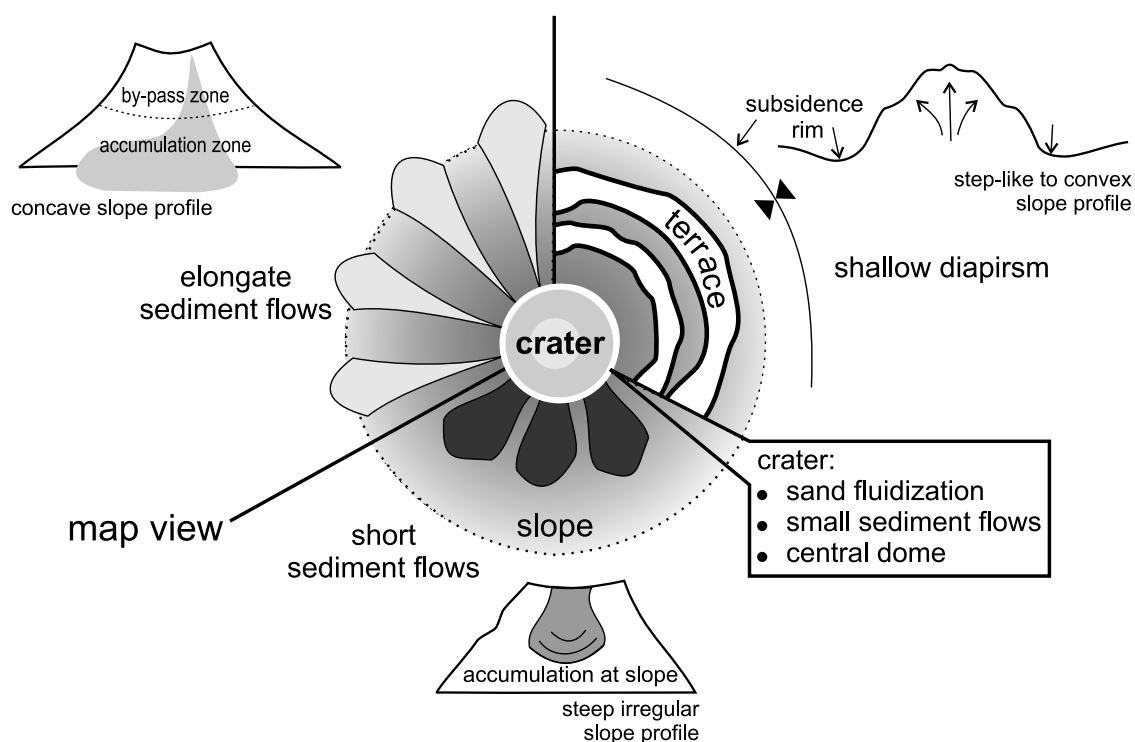


**Figure 12.** Interpretation drawing indicating the main sediment extrusion and intrusion processes and their resulting morphology. The slope morphology is shaped by different types of sediment flows and by uplift caused by sediment intrusion and diapirism. Within the crater the central dome is attributed to diapirism of low-density mud within the volcanic cone, whereas recent sediment extrusion created small debris flows, and fluidized sand flows were issued from secondary vents.

with subsidence rims. Subsidence rims around large mud volcanoes are a common feature at the Mediterranean ridge [Camerlenghi *et al.*, 1995], in the Gulf of Mexico [Prior *et al.*, 1989], at the Niger delta [Graue, 2000], and in the Gulf of Cadiz [Somoza *et al.*, 2002]. They are mostly attributed to collapse related to volume reduction caused by degassing, sediment removal or salt dissolution. However, also diapirs are often associated with a rim of synformal folding [e.g., Weinberg and Podladchikov, 1995; Harrison and Maltman, 2003] related to sediment withdrawal. However, more important subsidence probably takes place after mud volcano or mud diapir activity has ceased and dewatering occurs. Well-developed collapse depressions are found over abandoned mud volcanoes [Graue, 2000] and “deflated” diapirs [Morley and Guerin, 1996]. Somoza *et al.* [2002] on the other hand suggest that the moats are caused by erosional currents deflected by the mud volcano cone. In the El Arraiche field, the seismic data indeed indicate erosion in combination with subsidence. The subsidence rims do not evolve into sediment withdrawal synclines but are filled by

mud flows and layered hemipelagic sediments and reappear higher in the section at a slightly different position.

[34] Mud volcano feeder pipes were described as a network of sedimentary dykes by Morley [2003] and Van Rensbergen *et al.* [1999]. Dyke intrusions that reach the surface create vents. At present, vents seem to be restricted to the crater area. At Gemini mud volcano, at least 6 vents could be identified over a larger crestal area along an ENE-WSW orientation. It remains unclear whether large debris flows on the slopes were issued by vents within or outside the crater depressions. The observations at Gemini mud volcano seem to suggest the latter. Large flows occur at the eastern and western flanks in the continuation of the alignment of vents at the crest, and parallel to the mud volcano’s long axis, although the eastern and western slopes are not the directions of highest slope gradient. At the Mercator mud volcano, a single large mud flow seems to originate directly from the single vent at the crest of the central dome. At Al Idrissi mud volcano the crater is 17 m deep, yet the slopes are entirely covered by sediment flow

**Table 2.** Synthesis of the Measurements of the Main Morphological Elements of the Mud Volcanoes

	Overall Slope, deg	Steepest Slope, deg	Lowest Slope, deg	Max. Height Steps, m	Max. Width (Slope Parallel), m	Max. Length (Down Slope), m
Type I elongate mud flow	5–6	8–10	0.5–5	0–20	600–800	900–2500
Type II short mud flows	8–10	14–18	4–6	40–50	400–700	700–1400
Diapiric uplift?	8.2–10.5	12.5–13	2.5–6	30–45	400–1500	entire slope
Crater’s central dome	2.5–5	6–11	0	10–25	200–700	within crater
Sand fluidization				sand sheet within crater		

deposits. Were vents situated at the outside of the crater rim or did the crater subside later?

## 6. Conclusions

[35] The El Arraiche field is a cluster of 8 mud volcanoes situated below the shelf edge at the Moroccan margin. The largest mud volcano in the field (Al Idrissi mud volcano) is 255 m high and 5.4 km wide, the smallest we observed is only 500 m wide and 25 m high. The morphology of the mud volcanoes consist of, from base to top: a moat around part of the base of the mud volcano cone, an irregular slope characterized by radial outward sediment flows, terraces and/or depositional sediment flow escarpments (lobe fronts), a crater depression or a flat top, and a central dome.

[36] On basis of the observations we conclude that these large cone-shaped mud volcanoes result from a combination of intrusive and extrusive processes. Sediment flow deposits on the slopes range between two end-members. Flows with low yield strength (type I) extend to the base of the slope and create a steepening convex slope profile with a low overall slope angle ( $5^{\circ}$ – $6^{\circ}$ ). Flows with a high yield strength freeze on the steep slope and create an irregular slope profile with almost constant slope angle ( $8^{\circ}$ – $10^{\circ}$ ). Within the crater, several vents issue fluidized sand and small debris flows that consist of mud breccia with centimeter- to meter-sized clasts in a mud matrix. The extrusive sediment flows shape the surface of the mud volcano but in this study we also observe morphological elements that do not appear to correspond solely to extruded sediment deposits and may be partly result from sediment intrusion processes. The flat-topped central dome and the concentric pattern of continuous terraces and steps on the slope are interpreted to result from different phases of uplift by sediment intrusion, each possibly followed by collapse due to degassing or dewatering. Intrusive processes may involve shallow-seated diapirism caused by density reequilibration within the thick pile of remolded mud volcano sediments or uplift and volumetric expansion by injection of sedimentary dykes.

[37] **Acknowledgments.** The Belgica survey was part of the CADIPOR project, funded by the GOA project Porcupine-Belgica. The survey during TTR 12 was funded by a FWO research grant to PVR. PVR is funded by FWO-Flanders. DD is funded by IWT. The technical and scientific crew of R/V Belgica and R/V Logachev are gratefully acknowledged. Keith Lewis and Luis Pinheiro provided valuable comments in their reviews for JGR.

## References

- Annen, C., J.-F. Lénat, and A. Provost (2001), The long-term growth of volcanic edifices: Numerical modeling of the role of dyke intrusion and lava-flow emplacement, *J. Volcanol. Geotherm. Res.*, **105**, 263–289.
- Brown, K. M. (1990), Nature and hydrogeological significance of mud diapirs and diatremes for accretionary systems, *J. Geophys. Res.*, **95**, 8969–8982.
- Camerlenghi, A., M. B. Cita, B. Dellavedova, N. Fusi, L. Mirabile, and G. Pellis (1995), Geophysical evidence of mud volcanism on the Mediterranean Ridge, *Mar. Geophys. Res.*, **17**, 115–141.
- Déville, E., A. Battani, R. Griboulard, S. Guerlais, J. P. Herbin, J. P. Houzay, C. Muller, and A. Prinzhofer (2003), The origin and processes of mud volcanism: New insights from Trinidad, *Spec. Publ. Geol. Soc. London*, **216**, 381–394.
- Dimitrov, L. (2002), Mud volcanoes—The most important pathway for degassing deeply buried sediments, *Earth Sci. Rev.*, **59**, 49–76.
- Flinch, J. A. (1993), Tectonic evolution of the Gibraltar Arc, Ph.D. thesis, Rice Univ., Houston, Tex.
- Flinch, J. A., A. W. Bally, and S. Wu (1996), Emplacement of a passive margin evaporitic allochthon in the Betic Cordillera of Spain, *Geology*, **24**, 67–70.
- Gardner, J. M. (2000), Gulf of Cadiz/Moroccan margin: Mud diapirism and mud volcanism study, in *Multidisciplinary Study of Geological Processes on the North East Atlantic and Western Mediterranean Margins*, IOC Tech. Ser., vol. 56, edited by N. H. Kenyon et al., pp. 56–79, UNESCO, Paris.
- Gardner, J. M. (2001), Mud volcanoes revealed and sampled on the western Moroccan continental margin, *Geophys. Res. Lett.*, **28**, 339–342.
- Gràcia, E., J. Dañobeitia, J. Vergés, R. Bartolomé, and D. Córdoba (2003), Crustal architecture and tectonic evolution of the Gulf of Cadiz (SW Iberian margin) at the convergence of the Eurasian and African plates, *Tectonics*, **22**(4), 1033, doi:10.1029/2001TC901045.
- Graue, K. (2000), Mud volcanoes in deepwater Nigeria, *Mar. Petrol. Geol.*, **17**, 959–974.
- Harrison, P., and A. J. Maltman (2003), Numerical modelling of reverse-density structures in soft non-Newtonian sediments, *Spec. Publ. Geol. Soc. London*, **216**, 35–50.
- Henry, P., et al. (1996), Fluid flow in and around a mud volcano field seaward of the Barbados accretionary wedge: Results from Manon cruise, *J. Geophys. Res.*, **101**, 20,297–20,323.
- Hernández-Molina, F. J., L. Somoza, J. T. Vázquez, F. Lobo, M. C. Fernández-Puga, E. Llave, and V. Díaz-del Río (2002), Quaternary stratigraphic stacking patterns on the continental shelves of the southern Iberian Peninsula: Their relationship with global climate and palaeoceanographic changes, *Quat. Int.*, **92**, 5–23.
- Kenyon, N. H., M. K. Ivanov, A. M. Akhmetzhanov, and G. G. Akhmanov (Eds.) (2000), *Multidisciplinary Study of Geological processes on the North East Atlantic and Western Mediterranean Margins*, IOC Tech. Ser., vol. 56, 20 pp., UNESCO, Paris.
- Kopf, A., and J. H. Behrman (2000), Extrusion dynamics of mud volcanoes on the Mediterranean Ridge accretionary complex, *Spec. Publ. Geol. Soc. London*, **174**, 169–204.
- Maldonado, A., L. Somoza, and L. Pallarés (1999), The betic orogen and the Iberian-African boundary in the Gulf of Cadiz: Geological evolution, *Mar. Geol.*, **155**, 9–43.
- Morley, C. K. (2003), Outcrop examples of mudstone intrusions from the Jerudong anticline, Brunei Darussalam and inferences for hydrocarbon reservoirs, *Spec. Publ. Geol. Soc. London*, **216**, 381–394.
- Morley, C. K., and G. Guérin (1996), Comparison of gravity-driven deformation styles and behaviour associated with mobile shales and salt, *Tectonics*, **15**, 1154–1170.
- Mulder, T., and P. Cochonat (1996), Classification of offshore mass movements, *J. Sediment. Res.*, **66**, 43–57.
- National Geographic (Portuguese ed.) (2002), Combustível do Futuro? Margem sul nacional rica em vulcões de lama, Portuguese ed., **21**(1), 30.
- Pinheiro, L. M., et al. (2003), Mud volcanism in the Gulf of Cadiz: Results from the TTR-10 cruise, *Mar. Geol.*, **195**, 131–151.
- Prior, D. B., E. H. Doyle, and M. J. Kaluza (1989), Evidence for sediment eruption on deep-sea floor, Gulf of Mexico, *Science*, **243**, 517–519.
- Shih, T. T. (1967), A survey of the active mud volcanoes in Taiwan and a study of their types and the character of the mud, *Petrol. Geol. Taiwan*, **5**, 259–311.
- Somoza, L., V. Díaz-del-Río, J. T. Vázquez, L. M. Pinheiro, F. J. Hernández-Molina, and the TASYO/Anastasya Shipboard Parties (2002), Numerous methane gas-related sea floor structures identified in the Gulf of Cádiz, *Eos Trans. AGU*, **83**, 541.
- Somoza, L., et al. (2003), Seabed morphology and hydrocarbon seepage in the Gulf of Cádiz mud volcano area: Acoustic imagery, multi-beam and ultra-high resolution seismic data, *Mar. Geol.*, **195**, 153–176.
- Van Rensbergen, P., C. K. Morley, D. W. Ang, T. Q. Hoan, and N. T. Lam (1999), Structural evolution of shale diapirs from reactive rise to mud volcanism: 3D seismic data from the Baram delta, offshore Brunei Darussalam, *J. Geol. Soc. London*, **156**, 633–650.
- Van Rensbergen, P., J. Poort, R. Kipfer, M. De Batist, M. Vanneste, J. Klerkx, N. Granin, O. Khlystov, and P. Krinitsky (2003), Near-surface sediment mobilization and methane venting in relation to hydrate destabilization in Southern Lake Baikal, Siberia, *Spec. Publ. Geol. Soc. London*, **216**, 207–221.
- Van Rensbergen, P., et al. (2005), The El Arraiche mud volcano field at the Moroccan Atlantic slope, Gulf of Cadiz, *Mar. Geol.*, in press.
- Weinberg, R. F., and Y. Y. Podladchikov (1995), The rise of solid state diapirs, *J. Struct. Geol.*, **17**, 1183–1195.

D. Depreiter, J.-P. Henriët, B. Pannemans, and P. Van Rensbergen, Renard Centre of Marine Geology, Ghent University, Krijgslaan 281-S8, 9000 Gent, Belgium. (davy.depreiter@ugent.be; jeanpierre.henriet@ugent.be; happybappa@hotmail.com; pieter\_vanrensbbergen@yahoo.com)

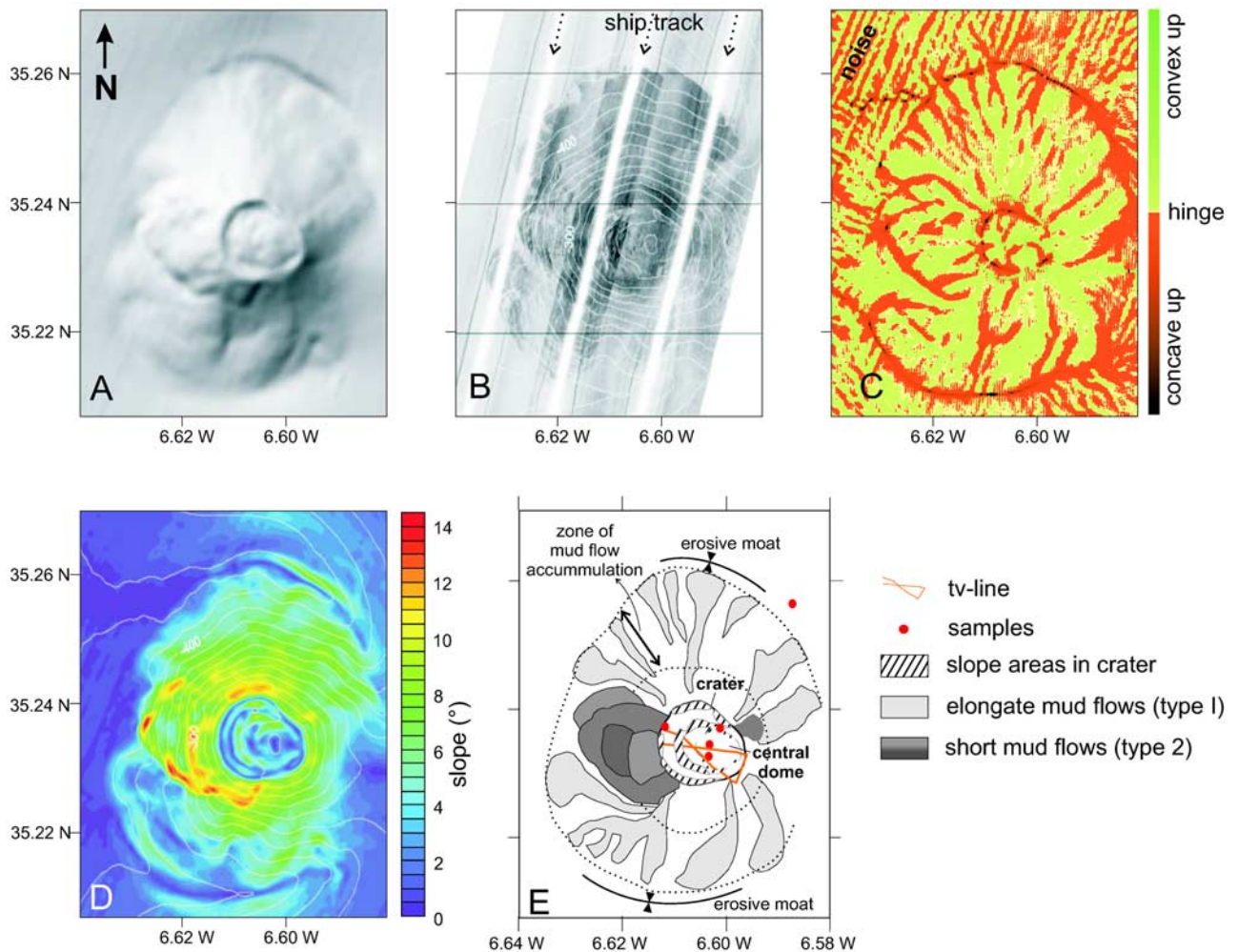


**Figure 5.** Morphology of the Al Idrissi mud volcano. (a) Shaded relief map. (b) Side scan sonar mosaic with bathymetry contours. (c) Curvature of mud volcano isobaths. (d) Slope map with bathymetry contours. (e) Interpretation map. Numerous sediment flow deposits, characterized by high backscatter and convex morphologies, are distinguished on the slopes. They occur in a radial pattern away from the crater and accumulate at the base of the volcanic cone (type I sediment flows), which results in a steepening, concave slope profile. On the western slope, sediment flow deposits accumulated at the slope (type II sediment flows) and created a steeper irregular slope profile.



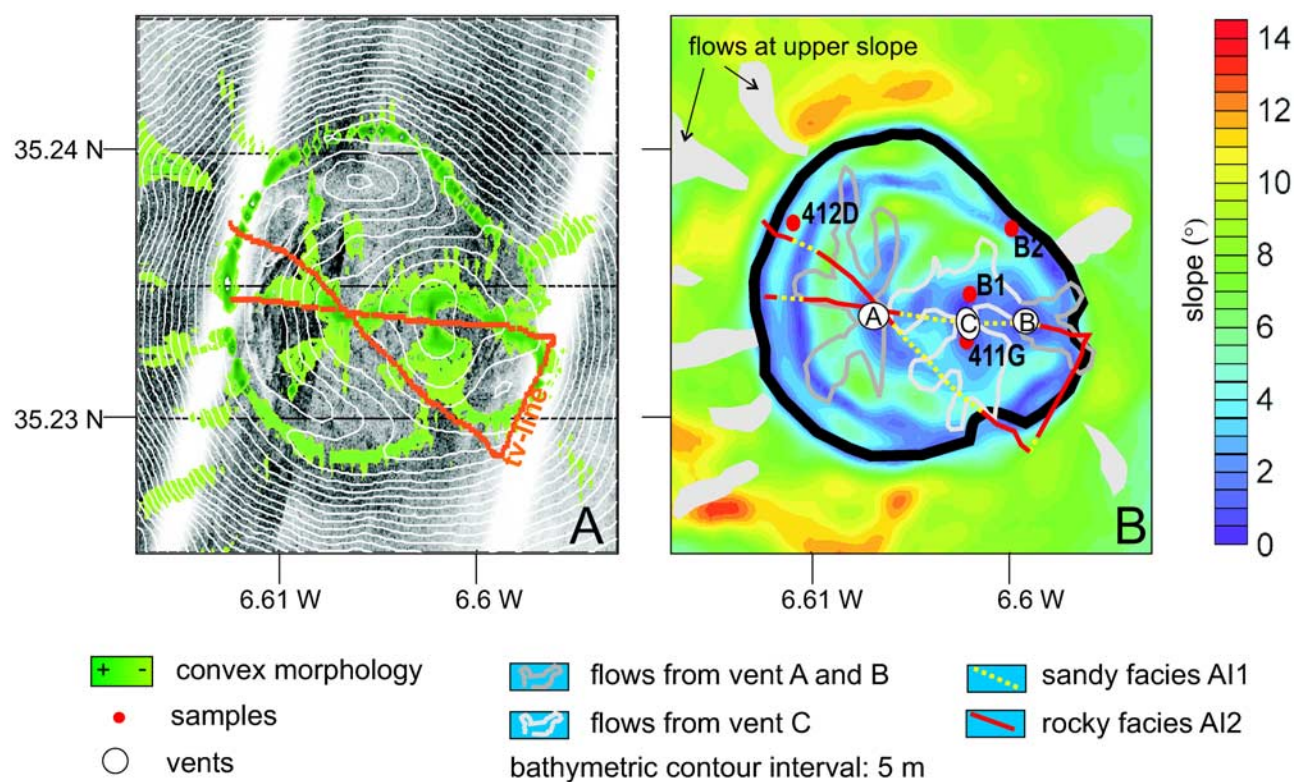


**Figure 6.** Crater of Al idrissi mud volcano. (a) Convex morphologies mapped over side scan sonar image shows the distribution of small mud flows issued by vents within the crater. (b) Slope map with indication of interpreted sediment flow deposits and sedimentary facies from underwater video lines distinguishing the different outflow events.

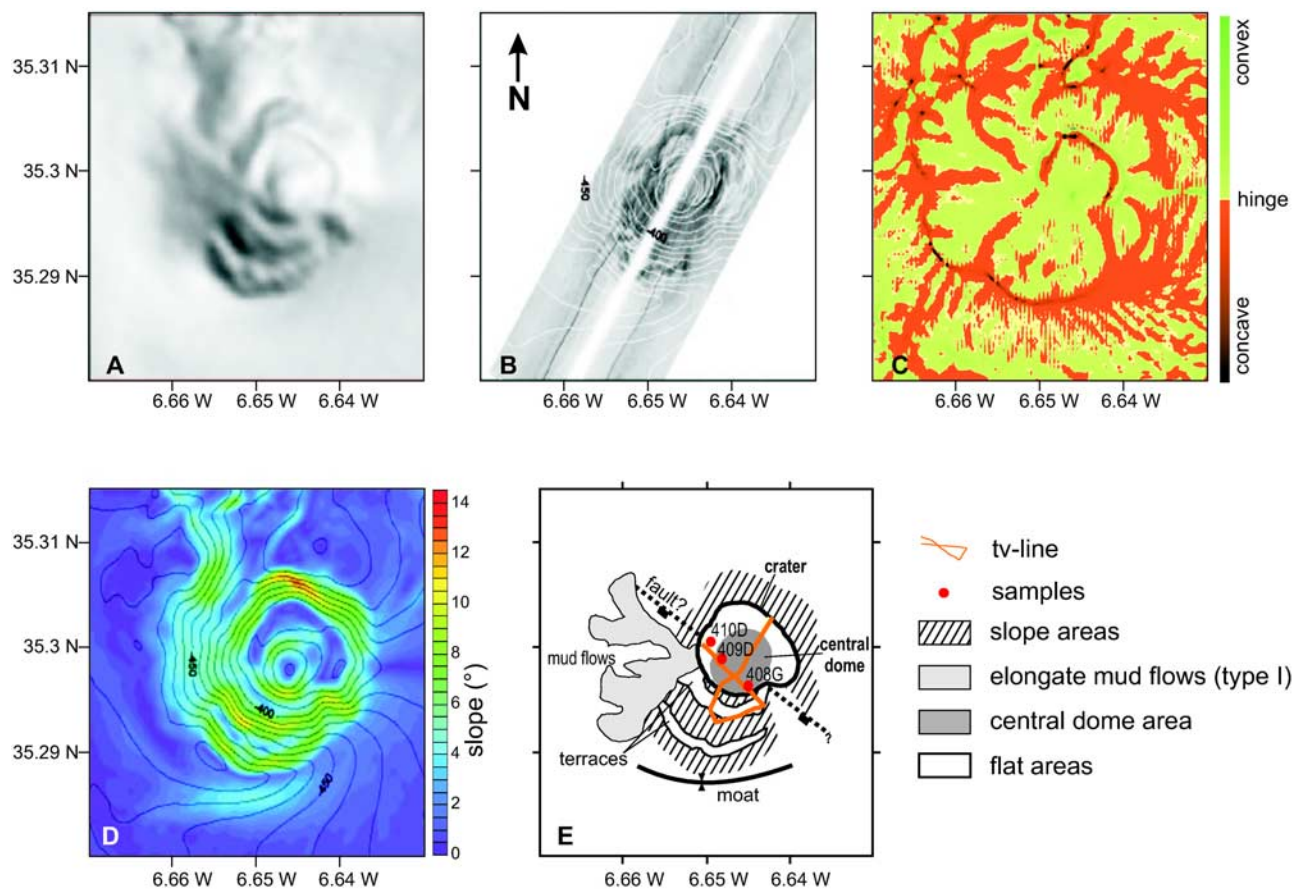


**Figure 8.** Morphology of the Mercator mud volcano. (a) Shaded relief map. (b) Side scan sonar mosaic with bathymetry contours. (c) Curvature of mud volcano isobaths. (d) Slope map with bathymetry contours. (e) Interpretation map. Mercator mud volcano is an asymmetric mud volcano with a smooth northern slope and concentric steps at the southern slope. Only at the western slope, type I sediment flow deposits, here characterized by a low backscatter, fan out at the base of the cone.

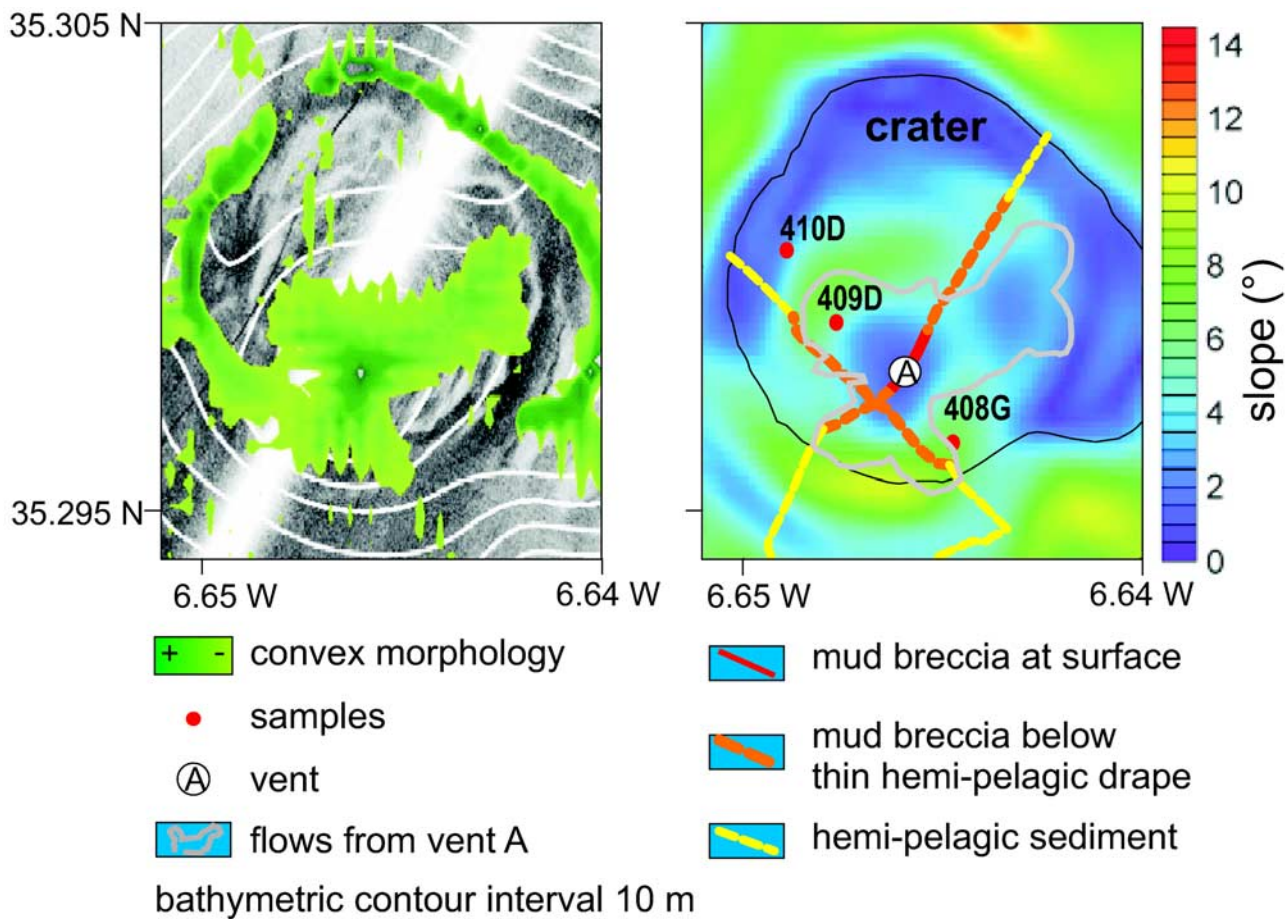


**Figure 9.** Crater of Mercator mud volcano. (a) Convex morphology mapped over side scan sonar image shows the distribution of small mud flows within the crater around a single vent at the summit. (b) Slope map with indication of interpreted sediment flow deposits and sedimentary facies from underwater video lines.



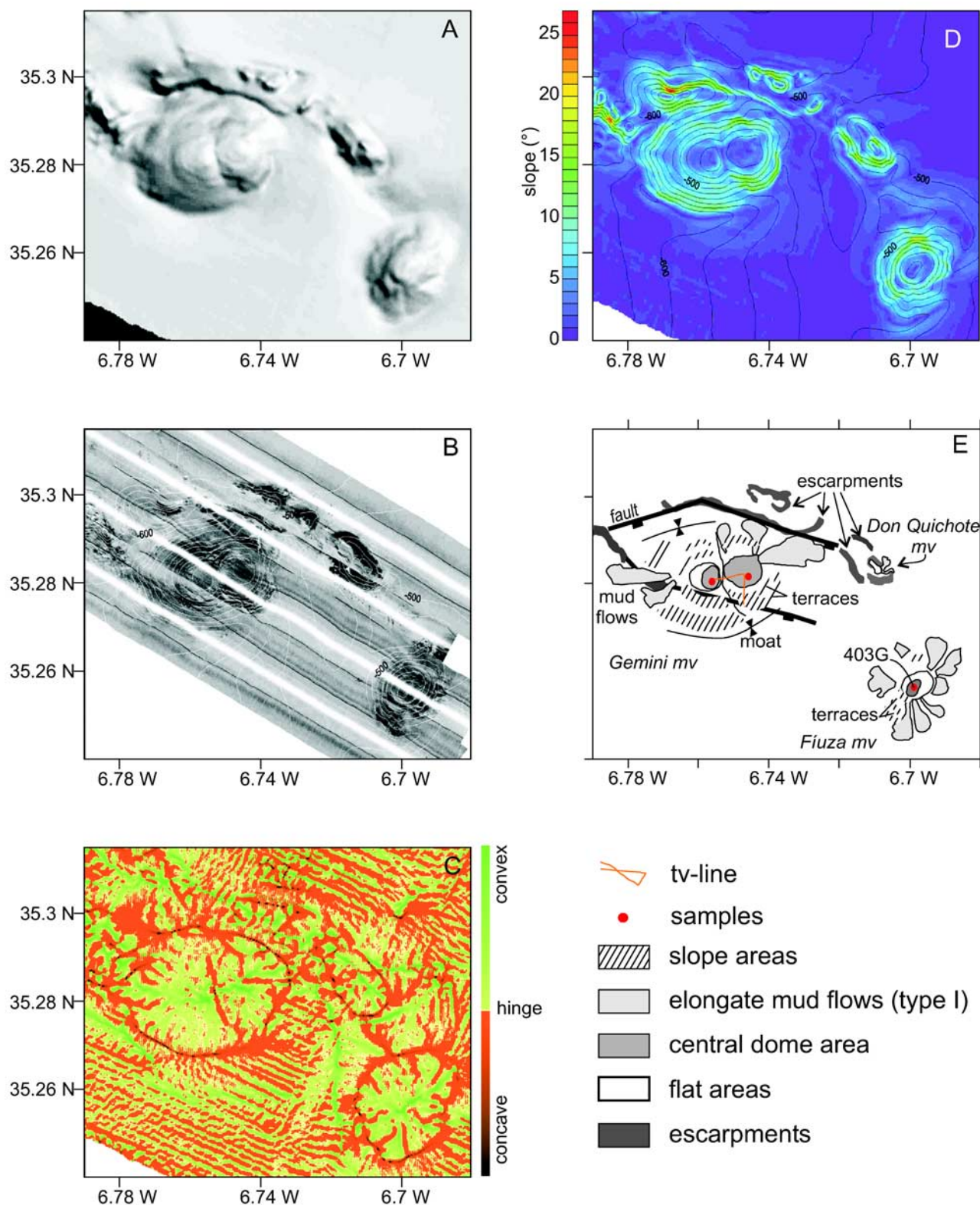


**Figure 10.** Morphology of Gemini and Fiuza mud volcanoes. (a) Shaded relief map. (b) Side scan sonar mosaic with bathymetry contours. (c) Curvature of mud volcano isobaths. (d) Slope map with bathymetry contours. (e) Interpretation map. Gemini mud volcano is a large oval-shaped mud volcano with two summits and an overall convex slope profile. The northern and southern flanks are steep with semiconcentric terraces. Type I sediment flow deposits at the base of the eastern and western slopes locally decrease the steep slope gradient. The flanks of the Fiuza mud volcano mainly consist of radial outward type I sediment flows that appear to mask a series of steps at the southern flank.

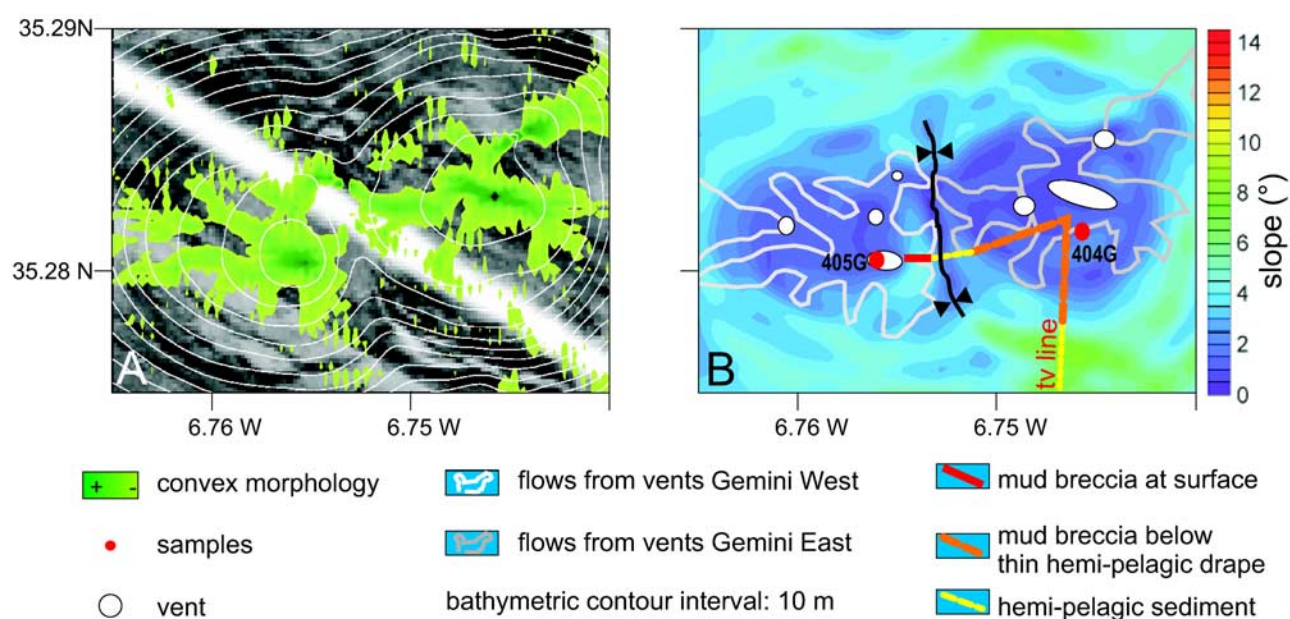


**Figure 11.** Crater of Gemini mud volcano. (a) Convex morphology mapped over side scan sonar image. (b) Slope map with indication of interpreted sediment flow deposits and sedimentary facies from underwater video lines. Up to seven vents have been identified at both summits. At the western summit, mud flow extrusion occurred recently.